DETERMINATION OF MECHANICAL PROPERTIES OF SILICON AND POLYMER MICRONEEDLES

A. Morrissey*, N. Wilke*, S.A.Coulman**, M.Pearton**, A.Anstey***, C.Gateley***, C.Allender**, K.Brain** and J.C.Birchall**

* Tyndall National Institute, Cork, Ireland
** Welsh School of Pharmacy, Cardiff University, Cardiff, CF10 3XF, UK.
***Gwent Healthcare NHS Trust, Royal Gwent Hospital, Cardiff Road, Newport, South Wales, NP20 2UB, UK.

nicolle.wilke@tyndall.ie

Abstract: The fabrication of polymer microneedles, using a silicon microneedle master, is presented in this paper. Silicon and polymer microneedles are used for drug delivery on skin and tumour therapy by electroporation. Single needle shear tests show the strength of microneedles depends on needle geometry, material and shear height. Mathematical evaluations of the shear strength were used to estimate shear forces during penetration into skin. Presented results of skin penetration show that less than 20% of needle tips broke very close to the tip after numerous periods of use. We can therefore suggest that also shear forces occur during penetration. Our microneedles are robust enough to be used for our applications.

Introduction

We have investigated the mechanical properties of silicon and polymer microneedles. Microneedles are commonly used for drug delivery or fluid extraction on skin, such as insulin infusion and blood monitoring. One of the main requirements for the use of microneedles in biomedical applications is the optimum ratio of microneedle fracture force to skin insertion force. Penetrated microneedles generate small channels through the stratum corneum, resulting in very highly efficient permeation. The mechanical characterisation of microneedles is very important and based on the requirements of strength, robustness, minimal insertion force and tissue damage in patients. Our microneedles are used in cancer therapy and the delivery of vaccines into skin. Both types of tissue are different in terms of material properties.

Materials and Methods

Silicon microneedles have been fabricated by wet and dry etch technologies. Wet etched microneedles with different tip radii have been fabricated using potassium hydroxide (KOH) [1]. Conical dry etched microneedles have been fabricated by dry etch technologies using SF_6/O_2, which was alternately used with the BOSCH deep reactive ion etch process [2]. Polymer microneedles are an alternative to silicon. Besides material properties, significant lower process costs and effort make them very interesting for medical applications. Therefore, silicon microneedles have been used as masters for micromoulding of a casting resin (Biresin® G36) for test purposes. The fabrication starts with a wet etched silicon master with microneedles formed below the wafer surface. The silicon is then completely embedded in silicone rubber (Sylgard ® 184 silicone elastomer curing agent, Dow Corning) following by degassing in a vacuum of 10^{-4} mbar (for at least 1 min). The vulcanization takes a minimum of 24 hours at room temperature with minimal shrinkage resulting in a specific Shore A hardness of about 42. The soft silicone mold is then used for vacuum casting. The dispensed liquid polymer (Biresin® G36 (resist) and Biresin® G36 (hardener), SIKA Deutschland GmbH, Germany) is introduced to a vacuum chamber (10^{-4} mbar, 1 min). The polymer parts are cured at room temperature for at least 24 hours, followed by heat treatment of 4 hours at 120°C in a convection oven. Using the mentioned polymers, the needle shapes of microneedles can be excellently reproduced. Figure 1 shows the different kind of needles, which have been used for shear and penetration tests.

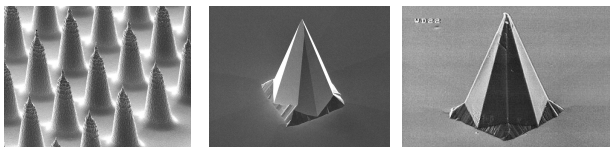

Figure 1: 250 μm tall dry etched needle (bottom diameter 200 μm) (left); 230 μm tall wet etched needle with base diameter of 180 μm (middle) and polymer needles (master wet etched needle(middle)) (right)

Silicon and polymer microneedles have been tested by single needle shear tests at a Royce 552 Instrument (Figure 2 left) and penetration tests into silicones (soft polymers) at a universal material testing machine (Instron 5500) by measuring the compression force (Figure 2 right). Soft polymers have been chosen in different thicknesses to model real tissue. Cling film layers have been used to model the skin layer on tissue.

ISSN: 1727-1983

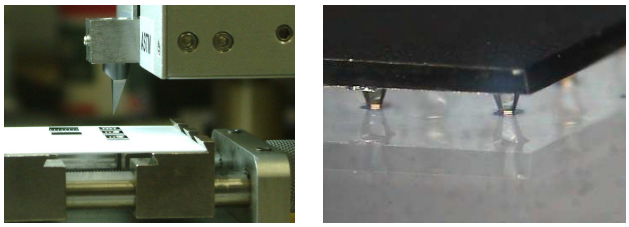

Figure 2: Setup for single needle shear tests (left); wet etched microneedle array penetrated into polymer (right)

Wet-etch microneedles have been mounted on steel rods (diameter 5-6 mm and length of about 2-2.5 cm) using epoxy resin and subsequently applied to human skin in a series of functional studies. Prior to microneedle application the skin is processed so that all the sub-cutaneous fat is removed and the skin is split. This involves pinning the skin onto a flat corkboard and carefully cutting the epidermis and upper region of the dermis, using a scalpel. The result is termed split thickness skin and is approximately 3 mm in depth. For microneedle application the split thickness skin is pinned over a semi-circular piece of cork. This ensures that sufficient tension is maintained in the skin, giving a more realistic representation of the *in vivo* state. Microneedle arrays were applied to the skin in a rolling motion.

Results

During penetration of microneedle arrays into tissue, two major issues must be addressed: the penetration force and the shear forces needles can withstand before breaking.

Single Needle Shear Tests

Measurements of single needle shear stress can be used to calculate the overall strength of microneedle arrays and to optimize needle geometry. Figure 3 shows the different shear behaviour of silicon and polymer microneedles. Silicon microneedles shear at the (111) crystal plane, which is known as the sliding plane with an angle of 54.74°. Polymer microneedles break in shear direction, due to its plastic behaviour.

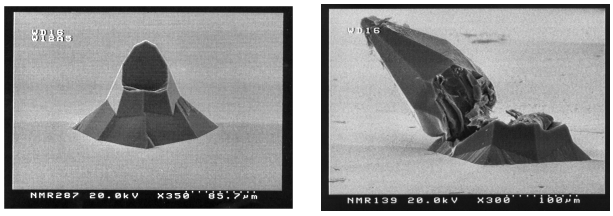

Figure 3: Result of single needle shear test on wet etched silicon (left) and polymer (right) microneedle

The force required to break a needle depends on the sheared area of the needle. Taller needles have larger base diameter, compared to smaller needles. The microneedle diameter of wet etched microneedles diminishes linearly between around 50 µm height and needle tip. Lower crystal planes, resulting in a wider diameter, form the base.

One can see in Figure 3 that higher forces are needed to break silicon microneedles compared to polymer microneedles. Silicon, even if it is brittle, is very hard. However, for shear heights >150 µm, measurements for polymer needles are close to the deviation of silicon microneedle results with the same shape. The wider sheared area along the (111) plane compared to sheared areas of polymer needles needs also be taken into account. The shear forces of dry etched microneedles decrease quite similarly to wet etched microneedles. Higher numbers are caused by larger aspect ratio of height : bottom diameter and therefore larger sheared areas. The wider base of wet etched microneedles due to lower crystal planes, results in higher forces to break the needle close to the ground. These results can have a positive influence when fully penetrated microneedle arrays are sheared in tissue.

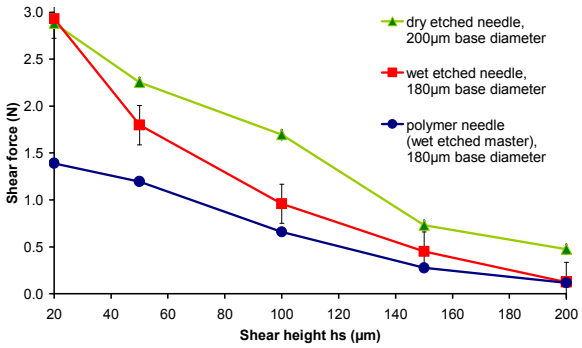

Figure 3: Shear forces for 3 different needle designs (see Figure 1) depending on shear height; standard deviations for dry etched and polymer needles are less than 100mN, for wet etched microneedles 300mN

In order to compare different needle designs independently from needle size, the shear strength σ_v needs to be calculated. Dimensions and forces are explained in Figure 4.

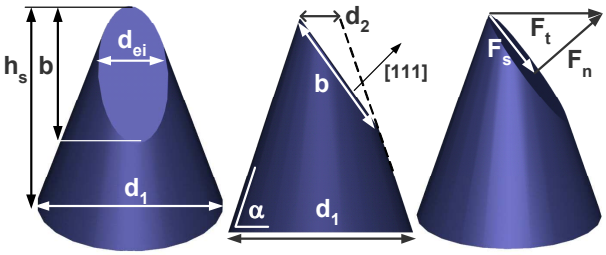

Figure 4: Model of sheared microneedle for shear strength calculation (3D AutoCAD drawing)

To calculate the normal stress σ_v for silicon microneedles, it is necessary to calculate the sheared area. The area is supposed to be an ellipse, which has

ISSN: 1727-1983

been adapted to the dimensions of the octagon (wet etched microneedle cross-section). The outer diameter d_n of the microneedle octagon, which is formed by high index crystal planes, is converted to a circle diameter d_1, where the circle area corresponds to the octagon area. The diameter d_1 is equal to the measured diameter of conical dry etched microneedles.

$$d_1 = 2 \cdot \sqrt{\frac{d_n^{\,2} \cdot \tan(54.74^\circ)}{\pi}} \tag{1}$$

The outer ellipse diameter b (d_{ei} is the inner ellipse diameter) depends on the base diameter d_1, the shear height h_s and the index h of the high index crystal planes.

$$b = \left(d_1 - \frac{2h_s}{h}\right) \cdot \frac{\sin(\arctan(h))}{\sin(\arctan(h) - 54.74^\circ)} \tag{2}$$

The sheared ellipse area A_E is given by

$$A_E = \cos(54.74^\circ) \cdot b^2 \cdot \frac{\pi}{4} \tag{3}$$

It has to be taken into account that polymer needles shear in shear direction (see Figure 2 right). The octagon area A_O is

$$A_O = \left(\frac{d_2}{2}\right)^2 \cdot \frac{n}{2} \cdot \cos(\alpha) = \left(\frac{d_2}{2}\right)^2 \cdot 4 \cdot \cos(45°) \tag{4}$$

With n the number of corners (here 8) and α the angle between the corners (here 45°).The diameter d_2 of the sheared area is

$$d_2 = d_n - 2 \cdot \frac{h_s}{h} \tag{5}$$

The shear strength of polymer needles is calculated by the shear force over the sheared area. The measured total force F_t for silicon needles needs to be split into shear force F_s and normal force F_n, which is the vertical force to F_s. Equation 6 gives the shear strength dependent on $F_s = \cos(54.74°) \cdot F_t$, $F_n = \sin(54.74°) \cdot F_t$ and the sheared area A_E.

$$\sigma_v = \frac{\sin(54.74^\circ) \cdot F_t}{2A_E} + \sqrt{\left(\frac{\sin(54.74^\circ) \cdot F_t}{2A_E}\right)^2 + \left(\frac{\cos(54.74^\circ) \cdot F_t}{A_E}\right)^2} \tag{6}$$

Shearing of silicon bulk material in lower shear heights, results in smaller sheared areas depending on the needle size. The ellipse area is not totally formed. The equations above can only be used when the sheared area is approximately an ellipse.

Figure 5 shows that the minimum shear height h_{sc} to get an elliptical area depends on the needle height and the base diameter respectively. The slope of the needle (given by index h) also has an influence on the sheared areas.

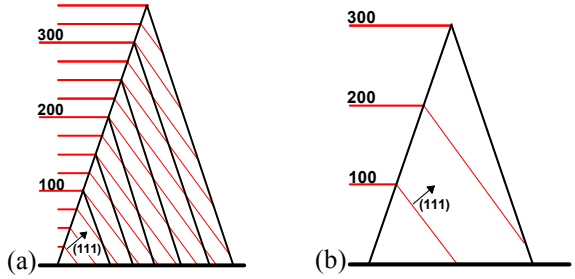

Figure 5: (a) General model of sheared crystal planes for different needle heights and h_s (Miller index h=3) for silicon microneedles, (b) explanation for h_s=100 and 200µm for 300µm tall needle

The comparison of shear strength for polymer and silicon needles can be seen in Figure 6. Due to the fact, that the sheared area is much smaller for polymer needles (6.2 times), the lower forces to break a needle (compare Figure3) result in higher shear strength. Figure 5 can be used as tool during the measurements, to see the approximated shear height for sheared areas only in the needle volume. The critical shear height $h_{s(c)}$ is given by

$$h_{s(c)} = \frac{\tan(54.74°) \cdot w}{1 + \frac{\tan(54.74°)}{h}} \tag{7}$$

with w, the base diameter of the microneedle and h the Miller index. For lower shear heights than $h_{s(c)}$ the sheared area decreases, but at the same time another area is created by breaking the needle out of the main volume of the silicon wafer. As a result, the shear force increases: (60±10) MPa for polymer, compared to silicon with (15±5) MPa. The diagram shows very clearly that the shear strength of dry etched microneedles is slightly higher compared to that of wet etched microneedles. The wider base and the higher angle of the sidewalls result in higher forces being required to break dry etched needles.

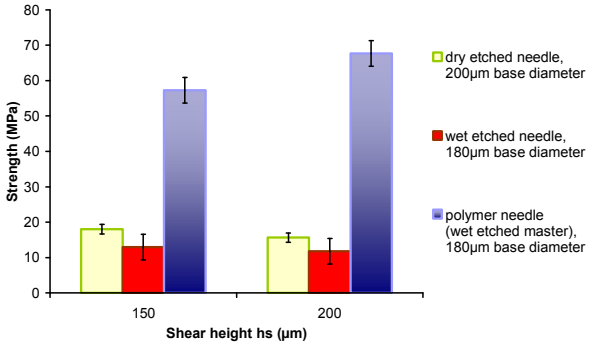

Figure 6: Shear strength for silicon and polymer microneedles, from measurements in Figure 3

ISSN: 1727-1983

Quanfang Chen measured a shear strength of 9.6 MPa for microstructures etched in 30% KOH [4]. He investigated that the shear strength is higher for dry etched (Reactive Ion Etching, RIE) structures compared to wet etched structures (using KOH). Our results are therefore in the range (and even higher) of the literature.

Hollow microneedle fluidic devices are very common. Drugs can be delivered, or blood extracted for example through the capillaries. Obviously the strength of the needle is afflicted due to the capillary. The following diagram illustrates the reduction of the sheared area for a hole, which is 66 µm in diameter and for this needle design (base diameter 190 µm) nearly half of the needle diameter. The needle walls are nearly 80° (index h=5.5) for those dry etched needles. It is assumed that the shear forces from the opposite side of the hole are reduced by the same amounts such as the area. It needs to be considered that the influence of the hole will increase with higher shear heights. In the real application such as drug delivery or cancer therapy, stress could be applied from different sides. Shearing the needle at the capillary side will result in even weaker behaviour.

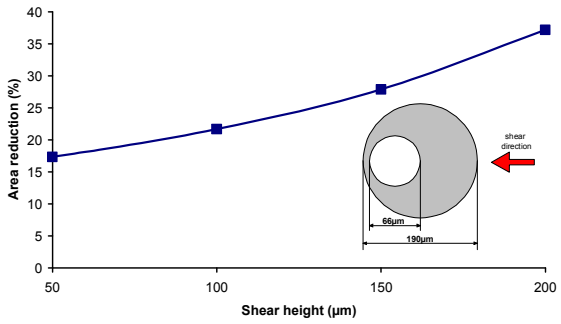

Figure 7: Area reduction for hollow dry etched microneedles referring to solid microneedles (base diameter 190 µm, needle height 250 µm, angle of walls 80°)

Penetration Tests into Soft Polymers

The dependency of needle geometry and penetrated material will be shown by penetration tests of wet etched silicon microneedle arrays into silicones (Figure 2) and skin. It is very difficult to model skin with polymers. However, it is known that the resistant upper skin layer, the stratum corneum, has a thickness of about 20 µm [5]. Cling film has more or less the same thickness and is elastic as well. The Shore hardness inside the thumb, which is often used for blood tests, is around 25 and therefore comparable to our model silicone of 2.7 mm thickness. The following results show that forces depend on:

- The thickness of the polymer
- Needle geometry
- Needle density / number of needles

One concern of silicon microneedles is that needle tip break and remain in tissue. Modifying the needle geometry to a frustum improves the strength as a result of wider areas which are sheared.

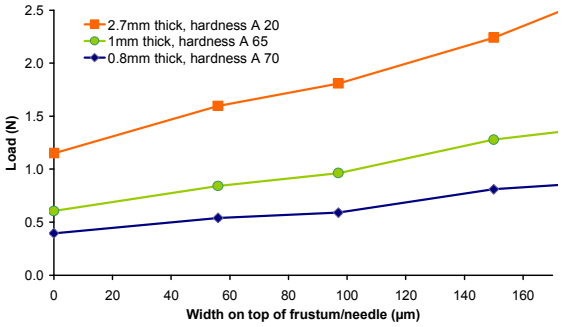

Figure 7: Penetration tests of solid silicon microneedle arrays into soft polymers (silicones), depending on needle geometry

On the other hand it will increase the area which penetrates into the tissue and therefore increases the force required to enter the tissue [6]. One can see in Figure 7 that penetration forces increase with a wider frustum width on top. Increasing the thickness of the silicone results in an increase in the elastic behaviour and can be illustrated by the relative Shore hardness. The decrease of the hardness causes an increase of penetration forces. The influence of the width on top of the frustum rises with decreasing hardness of the penetrated material.

The silicone has a certain mechanical resistance.The highest force during penetration is needed to enter the material [7]. Cling film layers have higher elastic behaviour than the used 2.7 mm thick silicone. Figure 8 illustrates very clearly that the way the needle array penetrates into the polymer increases with increasing number of cling film layers. That effect can be explained by dilatation of the cling film around the needle shape to a certain point where the needle tip scarifies the film and pushes into the silicone. It is interesting to mention that the Shore hardness of the silicone increases with increasing thickness of cling films and results in higher penetration forces.

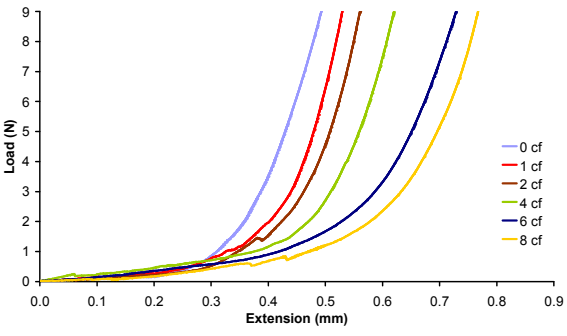

Figure 8: 2.7mm thick silicone (Shore hardness A 25) with different numbers of cling film on silicone (thickness 13µm)

ISSN: 1727-1983

Skin Penetration Tests

Frustum and pointed tipped microneedles have proven to be successful in the penetration of both heat separated (Figure 9) and full thickness human skin (data not shown).

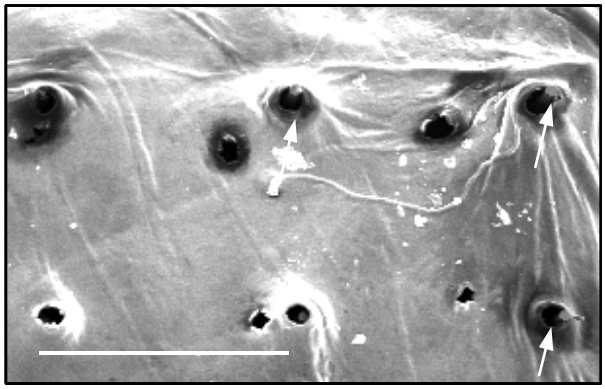

Figure 9: Scanning electron micrographs illustrating the ability of wet-etch microneedles with frustum-shaped tips to penetrate the epidermis; arrows highlight microneedle tips seen protruding through the human epidermal membrane Scale Bar = 1mm

However, visual inspection of the arrays (Figure 10), after repeated application to the skin, reveals the fragility of pointed microneedle arrays. Individual microneedles appear to splinter or break (Figure 11), most commonly at the microneedle tip, thereby rendering some needles incapable of puncturing the skin surface. Utilisation of the device within future studies, to create efficient and reproducible conduits for trans/intradermal delivery is therefore compromised when the microneedle arrays have to be used several times. Microneedles presented in Figure 11 have a base d_n of around 190 µm. The measured diameter d_2 (see Figure 4) was (30±10) µm. Using equations 1-3, the sheared area of 5532 μm^2 was calculated for an estimated shear height of 240 µm. The conversion of equation 6 to F_t is given by

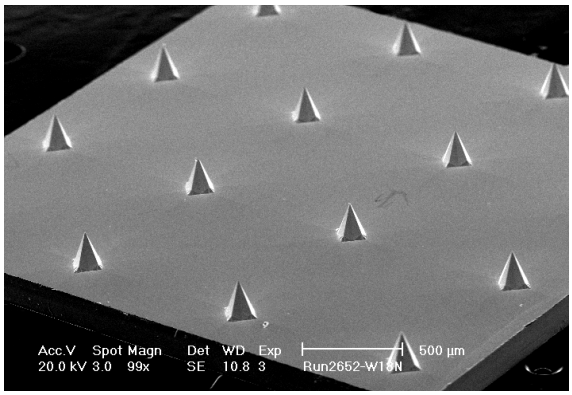

Figure 10: Scanning electron micrographs of wet-etch microneedle arrays

$$F_t = \frac{\sigma_v}{\frac{\sin(54.74°)}{2 \cdot A_E} + \sqrt{\left(\frac{\sin(54.74°)}{2 \cdot A_E}\right)^2 + \left(\frac{\cos(54.74°)}{A_E}\right)^2}} \qquad (8)$$

Applying the calculated sheared area and the shear strength of σ_v = (11.8±3.6) MPa (Figure 6), the total force F_t of (59.5±1.3) mN was applied while shearing the microneedle. Comparing those values with single needle shear test results, the shear height was approximately 217 µm. We assume that the shear force was applied from one side and therefore distributed over half of the perimeter of the octagon (47 µm). A point force, which could better be compared to single needle shear tests, is (1.3±0.03) mN. In case of one-dimensional vertical insertion of the microneedles into the skin, no shearing would occur. However, the results show that after repeated applications of the arrays to skin, shear forces can cause damage on needle tips, resulting in tiny silicon pieces of around 30 µm width remaining in the skin. Such shear forces occur while rolling flat microneedle arrays over skin, which is pinned over semi-circular pieces of cork. A circular microneedle device, such as the DERMAROLLER™ [9], can improve the penetration.

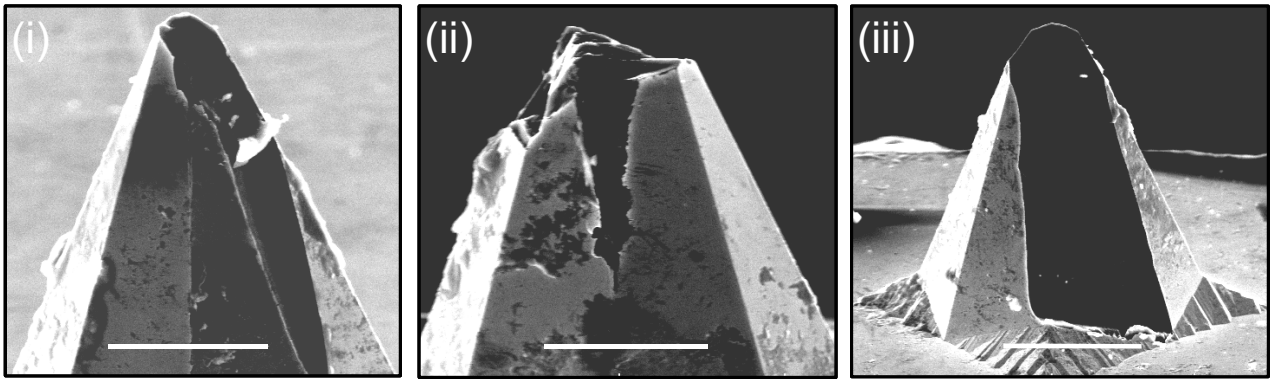

Figure 11: Scanning electron micrographs of wet-etch microneedle arrays. The Figure highlights the damage to microneedle tips following repeated insertions in to the human skin. (i), (ii) Scale Bar = 50 µm; (iii) Scale Bar = 100 µm

ISSN: 1727-1983

However, frustum shaped microneedles maintain their structure following repeated applications to the skin tissue (Figure 12). Such observations confirm the strength of the frustum-shaped microneedles, as predicted by the single needle shear tests. A notable feature of the frustum-shaped microneedles following application is the deposition of tissue around the microneedle tip. However, the integrity of individual microneedles can be restored simply by mechanical removal of the biological debris and the use of a detergent (Decon®).

Therefore, although a greater force is required for frustum-shaped microneedle tips to penetrate the skin surface, their robustness ensures penetrative reproducibility between experiments. It needs to be taken into account that the negative slope of the needle on top (presented in [3]), acts as a barb and can cause tissue damage. Corners could break during the withdrawal.

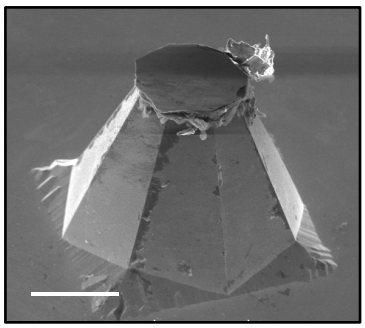

Figure 12: Scanning electron micrographs of wet-etch microneedle arrays; Figure illustrates the structural integrity of frustum-shaped microneedle tips following repeated insertions in to the human skin; Scale Bar = 100 μm

Summarizing the penetration tests of silicon microneedle arrays into skin, we affirm that microneedles with sharp tip as well as needle frustum shapes are suitable for penetration. Due to the fact that such arrays will not be used several times on patients, microneedles are robust enough for the treatment.

Conclusions

The mechanical characterisation of silicon and polymer microneedles in terms of biomedical applications was presented. Results of single needle shear tests show that polymer microneedles are as robust as wet etched microneedles. Due to the much smaller sheared area in shear direction, the shear strength itself has significantly higher values for polymer microneedles as compared to silicon microneedles. We demonstrated that the robustness of solid needles diminishes for hollow microneedles caused by the sheared area reduction. Penetration tests into soft polymers illustrate that the values are hardly comparable to skin due to a number of mechanical and geometrical influence factors. However, measured forces are close to literature values, where microneedles were penetrated into skin. Presented results of penetration tests into skin show that microneedles are very robust and suitable for delivery of vaccines. Microneedle arrays used for cancer therapy on tumours can also be used several times and do not break during mechanical cleaning with a soft brush (results not shown). Further penetration tests will be carried out with polymer and dry etched microneedles on skin.

Acknowledgements

This work was funded by Science Foundation Ireland (SFI) Research Frontiers Project (project number 05/RFP/ENG0063).

References

[1] WILKE N., MORRISSEY A., YE S. and O´BRIEN J.: 'Fabrication of microneedle arrays for drug delivery using wet etch technologies', Proceedings of European Micro and Nano Systems 2004, pp. 61-65

[2] WILKE N, HIBERT C., O'BRIEN J., MORRISSEY A.: 'Silicon Microneedle Electrode Array With Temperature Monitoring For Electroporation', *Sensors and Actuators A* ***xxx*** *(2005) xxx–xxx (in press)*

[3] WILKE N., MULCAHY A., YE S.-R., MORRISSEY A.: 'Process Optimization and Characterization of Silicon Microneedles Fabricated by Wet Etch Technology', *Microelectronics Journal* ***36*** *(2005) 650–656*

[4] CHEN Q., YAO D.-J., KIM C.-J., and CARMAN G. P., 'Influence of Fabrication and Crystal Orientation on the Strength of Silicon Microridges', ASME Int. Mechanical Engineering Congress and Exposition, Anaheim, CA. Nov. 1998., pp. 413-420

[5] ELIAS P.M., COOPER E.R., KORC A., BROWN B.E., 'Percutaneous transport in relation to stratum corneum structure and lipid composition', *J. Invest. Derm. 1981 Apr;****76****(4), pp. 297–301*

[6] HAIDER I., PETTIS R.J., DAVISON N., CLARKE R. and ZAHN J.D., 'Biomedical and Fluid Flow Characterization of Microneedle-Based Drug Delivery Devices', Proceedings of the 25th Annual Meetings of the American Society of Biomechanics, San Diego, CA, August 2001

[7] AGGARWAL P., JOHNSTON C.R., 'Geometrical effects in mechanical characterizing of microneedle for biomedical applications', *Sensors Actuators B* ***102*** *(2004), pp. 226–234*

[8] VERMA D.D. and FAHR A., 'Confocal laser scanning microscopy study using lipophilic fluorescent probe DiI incorporated in liposomes for investigating the efficacy of a new device for substance deposition into deeper layers of the skin: Dermaroller®'

ISSN: 1727-1983